

This is a preprint of a paper intended for publication in a journal or proceedings. Since changes may be made before publication, this preprint is made available with the understanding that it will not be cited or reproduced without the permission of the author.

RECEIVED  
LAWRENCE RADIATION LABORATORY

~~UCRL-70247 Rev. 1~~  
**PREPRINT**

SEP 15 1967

TECHNICAL INFORMATION DIVISION  
LIVERMORE

**Lawrence Radiation Laboratory**

UNIVERSITY OF CALIFORNIA

LIVERMORE

SHOCK-WAVE STUDIES IN CONDENSED MEDIA

R. E. Duff

W. H. Gust

E. B. Royce

A. C. Mitchell

R. N. Keeler

W. G. Hoover

September 1, 1967

This paper was prepared for publication in Proceedings of the IUTAM Symposium on Behavior of Dense Media Under High Dynamic Pressures, Paris, France, September 11-15, 1967

# SHOCK-WAVE STUDIES IN CONDENSED MEDIA\*

R. E. Duff, W. H. Gust, E. B. Royce, M. Ross, A. C. Mitchell  
R. N. Keeler, and W. G. Hoover

Lawrence Radiation Laboratory, University of California  
Livermore, California

## INTRODUCTION

This paper is an experiment. We have tried to lump together several pieces of research into a single paper in the hope that we could convey some idea of the work underway at our Laboratory. Obviously, the discussion of each topic will be sketchy, but we hope it will alert those interested in some particular subject to watch for the detailed account of each investigation when it is published in due course.

## EQUATION-OF-STATE MEASUREMENTS ON RARE-EARTH METALS AND THEIR IMPLICATIONS

Over the years shock-wave Hugoniot measurements have been made for a very large number of substances, but the rare earths and yttrium and scandium had escaped close scrutiny. This is surprising in view of the known peculiarities of these elements. We decided to investigate nine rare earths chosen to span the lanthanide series, plus yttrium and scandium which have similar physical properties.

The elements chosen and their atomic numbers are shown in the following table. An S behind the atomic number means that this element was also recently investigated by Al'tshuler et al. (1).

Scandium	21	Samarium	62 S
Yttrium	39	Europium	63
Lanthanum	57 S	Gadolinium	64
Cerium	58 S	Dysprosium	66 S
Praseodymium	59	Ytterbium	70
Neodymium	60		

Shock and free-surface velocity measurements were made on 6.4- and 3.2-mm-thick samples by well-known optical flash-gap techniques. The experimentally determined shock and particle velocities for several of the elements are summarized in Fig. 1. The results from the Soviet group which can be compared with our measurements are also included in Fig. 1. It is clear that the two investigations are in substantial agreement, but some differences do exist. Note that the initial shock compressibility for these rare-earth elements is high (low intercept and slope in the  $U_s - U_p$  graph). Furthermore, the  $U_s - U_p$  lines are not straight. Therefore, these materials

\*Work performed under the auspices of the U. S. Atomic Energy Commission.

are characteristically different from the majority of other elements that have been investigated.

A careful look was taken at the systematics of atomic compressibility as revealed by shock-wave measurements (2) with special attention paid to the rare earths. The changes in atomic radii as a function of pressure at 0° K show that s-electron bonded metals (the alkali and alkali earth elements) are relatively more compressible than the d-electron bonded metals. All of the rare earths except europium and ytterbium are normally d-bonded. The above correlation suggests that they should be relatively incompressible, contrary to observation. It is, therefore, concluded that the 5d electron in these rare earths is promoted to the unfilled 4f level at quite low pressures. This promotion would mean that rare earths would then become s-bonded. The observed compression of these elements agrees well with the compression of their s-orbitals. This is determined by scaling the Z dependence of the radius of the orbital for s-electron metals and rare earths as determined from Hartree-Fock calculations.

The conclusion is strengthened by two additional observations. At high pressure, all of the rare earths have essentially the same density. The large density difference between the normally d-bonded rare earths and the s-bonded rare earths europium and ytterbium is completely eliminated. In addition, yttrium and scandium, the elements above lanthanum in the periodic table, are d-bonded and have no f-levels energetically available to accept the d-electrons. They are incompressible as expected.

This reasoning may explain the high initial compressibility of the rare-earth metals, but it does not explain the decrease in compressibility at high pressure. This is thought to be caused by the closed 4p xenon shell which is observable in this case because the rare earths are d-bonded at zero pressure and are, therefore, relatively dense. The combination of abnormally high initial density and high initial compressibility leads to atomic volumes sufficiently small at readily attainable shock pressures for the closed inner shell of electrons to influence the interatomic forces. We have observed a similar stiffening of the Hugoniot for yttrium; Bakanov and Dudoladov (3) have seen the effect for calcium and strontium. This stiffening appears to occur when the closed-shell atomic cores first start to overlap. Therefore, the decrease in compressibility may arise from repulsion of closed electron shells though it occurs at a smaller core overlap than that characterizing the stiffening in the rare earths.

The Soviet group has proposed that these breaks in the Hugoniot of the rare earths and of calcium and strontium are the result of a promotion of an electron to a d-level in a second-order phase transition. This seems unlikely, since any significant population of a d-level at these large compressions appears to be energetically unfavorable, as one can estimate from the cohesive energy curves for typical d-electron bonded metals.

#### ELECTRONIC BAND STRUCTURE CALCULATIONS AND EQUATIONS OF STATE

As part of the overall program in the study of equations of state at high pressures, the inert gases, argon and xenon, have been shock-compressed to

two and three times their normal liquid density (4). These experiments were theoretically analyzed, using the Monte Carlo method, and a repulsive intermolecular potential for argon was determined and shown to be in good agreement with results obtained from molecular beam methods (5). If one applies the law of corresponding states to the Hugoniot and scales the argon measurements to the xenon measurements, it is found that below 200 kbar the two sets of data are in very good agreement. However, above this pressure the xenon points lie significantly below those of argon in the P-V plane. These results are shown in Fig. 2, where solid curve A is the averaged argon experimental results scaled up to xenon, and the dashed extension is an extrapolation of the theoretical curve which fits the entire Hugoniot. The disagreement between the two Hugoniot at high pressure is probably related to differences in electronic excitation in the two cases. Because of the high temperatures generated and the fact that the first excited state of xenon (8.4 eV) is significantly lower than argon (11.5 eV), xenon will undergo considerably more electronic excitation than argon, and its Hugoniot will be softer. In order to place these qualitative ideas on a more quantitative basis, energy band calculations have been made for both materials as a function of compression.

The energy band calculations show that at the highest xenon pressures the energy gap between the valence and conduction band has narrowed about 2 volts, and the 5d-like conduction bands now lie below the 6s, as is the case in compressed cesium. Using the results of these band calculations, a theoretical Hugoniot curve, B in Fig. 2, has been obtained which is in agreement with the xenon experimental curve. At the highest point on the xenon Hugoniot the temperature is near 2 eV, and the energy gap is about 6 eV. Therefore, electrons from one atom in five are promoted into the conduction band. Under these conditions xenon becomes metal-like, even though a large band gap still exists.

## ELECTRICAL CONDUCTIVITY STUDIES

Measurements of electrical conductivity of shock-compressed substances have been made in many laboratories, including our own (6-9). Unfortunately, the scatter of the data is rather larger than one would like to see. This led us to investigate the problems of making conductivity measurements and to determine their solutions. It has also led to some excellent data on the conductivity of shock-compressed liquid carbon tetrachloride between 70 and 160 kbar and of liquid xenon at 150 kbar.

Several experimental factors must be taken into consideration in measuring conductivity in shocked media between parallel plane electrodes. The field lines surrounding the conductivity electrode will not, in general, be one-dimensional. To account for this, a fringing field correction must be applied. The sample and electrode dimensions must be such that the effect of lateral rarefactions behind the shock front is minimized. The conductivity electrode must be a close shock-impedance match to the sample to minimize the reflected shock and rarefaction waves. The shock-wave motion should be normal to the surface of the conductivity electrode if the effects of the residual reflected shocks and rarefactions on the conductivity measurements are to be easily calculated. Allowance must be made for the attenuation of the initial shock wave and the decreasing pressure behind the shock front. The error in

determining conductivity as a function of pressure depends on the pressure measurement as well as the conductivity measurement, and these errors must be included in the data analysis. There will be a capacitance effect caused by the movement of the shock front relative to the electrode face. This will generate a voltage which begins when the shock wave enters the sample and increases as the shock front approaches the conductivity electrode. Shock tilt relative to the electrode face and this capacitance effect will reduce the rise time of the conductivity signal and perhaps reduce the accuracy of the measurement. Circuit response is limited by the presence of stray-shunt capacitance. All these factors must be considered if accurate conductivity measurements are to be made.

The fact that precise conductivity measurements can be made is illustrated by Fig. 3 which shows a plot of experimental data for carbon tetrachloride shocked between 70 and 160 kbar. The data cover seven orders of magnitude in conductivity, and the equation-of-state measurements contribute the major uncertainty to the data. It most certainly is necessary to correct the measurements for wave attenuation and electric fringing fields if precise (10%) data are to be obtained.

The shock-impedance matching problem turned out to be particularly important, as is illustrated in Fig. 4 which shows experimental records taken with anvils of different shock impedance. The calcium is an excellent match, while magnesium, aluminum and copper produce progressively higher shock impedances. In each case the slow rise of the signal is caused by the capacitance change as the shock front approaches the electrode. The signal rise at later time in the metal anvil experiments is caused by increased conductivity behind the shock reflected from the anvil itself. It is clearly difficult to estimate the conductivity of singly shocked  $\text{CCl}_4$  from the aluminum record, and it becomes more so if even higher impedance electrodes like copper are used. In fact, if the lower flat part of the Cu anvil trace were read as the singly shocked state, an error of two orders of magnitude in conductivity would be made. We suggest that a significant part of the scatter in previously published data may have arisen from insufficient attention to these details.

These experimental techniques have been applied to liquid xenon because equation-of-state measurements (4) and the calculations mentioned above suggest that electronic excitation makes a significant contribution to its energy above shock pressures of 300 kbar. At 150 kbar, the measured conductivity is  $0.1/\Omega$  cm. Experiments are continuing.

The experimental techniques appropriate for  $\text{CCl}_4$  and liquid xenon are not appropriate for metals. We have begun conductivity measurements of metallic foils by looking at shock-induced resistance changes by methods similar to those suggested by Fuller and Price (9). Figure 5 shows experimental records for copper and iron. The copper record is as expected, showing increased resistivity upon shock arrival  $0.3 \mu\text{sec}$  after the start of the record. The iron trace shows much more structure. The high-voltage spike is not an instrumental artifact. It is a manifestation of the shock-induced demagnetization of iron that occurs above the 130-kbar transition. Before the shock arrives, a relatively large magnetic field within the wire is induced by the resistance-measuring current. The shock demagnetizes the wire, and

the original magnetic field can no longer be supported by the current in the wire. Therefore, eddy currents are induced which dissipate the magnetic energy. The currents generate a voltage spike which superficially indicates that iron has a negative resistance. The decay of the voltage pulse is governed by the conductivity of the wire. The conductivity deduced from the transient signal is in good agreement with the value indicated on the same record after the decay of the transient. This observation provides dramatic proof of the non-magnetic nature of  $\epsilon$ -iron. The step change in voltage before the spike is caused by the arrival of an elastic wave in  $\text{Al}_2\text{O}_3$   $\mu\text{sec}$  in which the sample was buried. It appears that demagnetization is occurring at a slow rate at a pressure of 80 kbar.

### OPTICAL TECHNIQUES

Modern nonlinear optical techniques have been successfully applied in shock-wave experiments. Stimulated Brillouin scattering has been carried out in shock-compressed fluids, with the experimental configuration shown in Fig. 6 (10). The three-laser system provided a spectrally pure, 20-nsec pulse, timed to arrive behind the shock front just before the shock wave reached the lens. This experiment provided a value of the velocity of sound in acetone, shock-compressed to 35 kbar, 31% compression, and  $910^\circ\text{K}$ . The velocity of sound was calculated from the modified Brillouin formula,

$$\Delta\nu' = \frac{2\nu_0}{C} \left\{ n_2 v_s + (n_2 - n_1) U_s - n_2 U_p \right\}.$$

Here  $\Delta\nu'$  is the downward shift in frequency of the back-scattered light as determined from the Fabry-Perot interferometer,  $n_2$  is the refractive index in the shocked medium, and  $n_1$  is the refractive index in the unshocked medium.  $U_s$  and  $U_p$  are the shock and particle velocity, and  $v_s$  is the velocity of sound. The measured value of sound velocity obtained agreed with the theoretical velocity within experimental accuracy (about 5%).

Having shown the feasibility of carrying out such experiments, we are presently developing a simpler, more reliable laser oscillator to produce single-mode pulses 20-40 nsec in duration, timed to better than  $0.1 \mu\text{sec}$ . This system should make possible measurement of the velocity of sound at hypersonic frequencies, determination of transport properties in shocked transparent materials, and direct Doppler measurements of particle velocity.

Other laser techniques will undoubtedly provide valuable tools for the measurement of free surface velocity. The paper by Barker at this meeting provides an excellent illustration. Workers in another part of our Laboratory (11) have developed a somewhat similar system which uses a short, low-finesse Fabry-Perot interferometer as the frequency demodulation detector of Doppler-shifted laser radiation. In this system, velocity is indicated by a change in transmission coefficient of the interferometer. The interferometer filling time is small compared to 1 nsec, and the system can be designed to measure surface velocities in any velocity range. This tool will be useful in studies of phase transitions and elastic-plastic phenomena.

## PHASE TRANSITION STUDIES

Shock-induced phase transitions have been observed in many laboratories with many different techniques. We have undertaken a modest effort to redetermine several observed transition pressures so as to provide more reliable values for the calibration of static high-pressure scales, and to provide more definitive tests of the equivalence of static and dynamic compression where really firm static data exist.

A redetermination of the pressure of the lowest bismuth transition, using quartz gage techniques, has demonstrated (12) excellent agreement between static and dynamic determinations if the elastic precursor present in the dynamic case is properly taken into account. Internally reflecting prisms (13) have been used to determine the phase transition in tin. In this case we have shown that the elastic wave contribution is very small. Our value of 94 kbar is in excellent agreement with the currently accepted static value of 92 kbar, but the temperature of the shocked sample should be determined before such comparisons are made. The calculations of McQueen suggest that tin shocked to 94 kbar has a temperature of approximately 190°C. The work of Kennedy (14) and Barnett (15) suggests that the white tin - tin II transition pressure is 75 kbar at 190°C. This 25% disagreement between the static and dynamic determinations of phase transition pressure in tin is a source of concern.

It has been proposed that post-experimental, metallographic observation of whether or not a phase transition had occurred in a Fe-Ni-Cr alloy could provide a rough measure of the pressure to which a system was subjected. The transition pressure for several alloy compositions has been measured by pin techniques (16), but it seemed desirable to verify the measurements by the inclined mirror method.

Figure 7 summarizes the results. Qualitatively, the agreement between the two sets of experiments is good except for the 18-8 stainless steel and the 30% Cr alloy. We find the transition pressure for the stainless steel to be more than a factor of two higher than the value previously reported. It appears that a relatively large elastic wave may have been mistaken for the transition wave in the earlier work.

## SHOCK WAVE STRUCTURE

The detailed structure of a shock wave has received considerable attention over the years. The Navier-Stokes equations, the Mott-Smith bimodal distribution function, and more fundamental kinetic theory approaches have been exploited to produce a good understanding of shock structure in gases. The situation is much less satisfactory in dense fluids and solids where analyses based on the binary-collision Boltzmann equation cannot be trusted. However, it is not unreasonable to assume that the shock transition in an ideal solid would be quite thin. If this were so, the transition could probably be investigated by the numerical techniques of molecular dynamics. Such an investigation is underway.

In a molecular dynamics calculation the coordinates and velocities of a limited number of particles are specified, along with boundary conditions which hopefully minimize the small-system distortions. The particles are then

advanced under constraints imposed by the assumed force laws between them. The calculation is continued until statistical fluctuations have been averaged out. In the shock-wave problem, the propagation direction is singled out for special treatment. Periodic boundaries normal to the propagation direction simulate an infinite medium. Along the direction of shock propagation, a coordinate system centered on the shock wave is used. Particles enter at the low-density, low-temperature side at the shock velocity. They leave at the other side, the hot side, at a velocity equal to the shock speed minus the particle speed. The whole system needs only to be long enough for the conversion from initial to final states to take place well away from the boundaries where new particles are fed in and old ones discarded.

To obtain a precisely fixed shock front, one must correlate the properties of the incoming stream of particles with those of the outgoing stream. To do this, it would in principle be necessary first to compute the equation of state, and then to solve the conservation equations to match the input and output streams. In practice, an approximate match resulting in shock-front drift can be used; the drift can then be halted by adjusting the output stream velocity.

The molecular-dynamic technique just outlined has been applied to the two-fold compression of a face-centered cubic crystal composed of particles interacting with a potential which varies as the inverse twelfth-power of the distance between each pair of particles. The lattice is initially at 0°K. Preliminary results show that the shock transition, in terms of distance separating the low-velocity and high-velocity streams, is only about three lattice parameters thick. The transition appears to be stable, and independent of the total length of the system. The state behind the shock appears to be a hot, disorganized fluid. Still to be studied is the dependence of shock structure on the direction of propagation through the crystal and on the interparticle force laws. It is expected that these studies will lead first to an accurate molecular picture of shock structure under a variety of conditions, and then to a unifying theoretical treatment valid for high-density systems.

## REFERENCES

- (1) L. V. Al'tshuler, A. A. Bakanova, and I. P. Dudoladov, *Zh. Eksper. Theor. Fiz., Pisma v Redakt.* 3, 483 (1966) [Eng. Tr. JETP Letters 3, 315 (1966)].
- (2) E. B. Royce, Stability of the Electronic Configuration and Compressibility of Electron Orbitals in Metals as Determined from Shock Wave Data, Lawrence Radiation Laboratory Report UCRL-50102, November 21, 1966.
- (3) A. A. Bakanov and I. P. Dudoladov, *Zhur. Expt. i. Theor. Fiz Pisma* 5, 322 (1967) [Eng. Tr. JETP Letters 5, 265 (1967)].
- (4) R. N. Keeler, M. van Thiel and B. J. Alder, *Physica* 31, 1437 (1965).
- (5) M. Ross and B. J. Alder, *Chem. Phys.* 46, 4203 (1967).
- (6) B. J. Alder and R. H. Christian, *Discussions Faraday Soc.* 22, 44 (1956).
- (7) L. V. Al'tshuler, L. V. Kuleshova and M. N. Pavolovskii, *JETP* 39, 16 (1960) [Eng. Tr. Soviet Phys. JETP 12, 10 (1961)].
- (8) S. D. Hamann and M. Linton, *Trans. Faraday Soc.* 62, 1 (1966).
- (9) P. J. A. Fuller and J. H. Price, *Nature* 193, 262 (1962).

(10) R. N. Keeler, G. H. Bloom and A. C. Mitchell, *Phys. Rev. Letters* 17, 852 (1966).

(11) T. Burgess, private communication.

(12) D. B. Larson, *J. Appl. Phys.* 38, 1541 (1967).

(13) G. Eden and P. W. Wright, *Fourth Symposium on Detonation*, U. S. Government Printing Office, (1965), p. 573.

(14) G. C. Kennedy and R. C. Newton, *Solids Under Pressure*, W. Paul and D. M. Warschauer, Eds. (McGraw-Hill Book Co. Inc., New York, 1963) p. 163.

(15) J. D. Barnett, R. B. Bennion and H. T. Hall, *Science* 141, 1041 (1963).

(16) C. M. Fowler, F. S. Minshall and E. G. Zukas, *Response of Metals to High-Velocity Deformation* (Interscience, New York, 1961) p. 175.

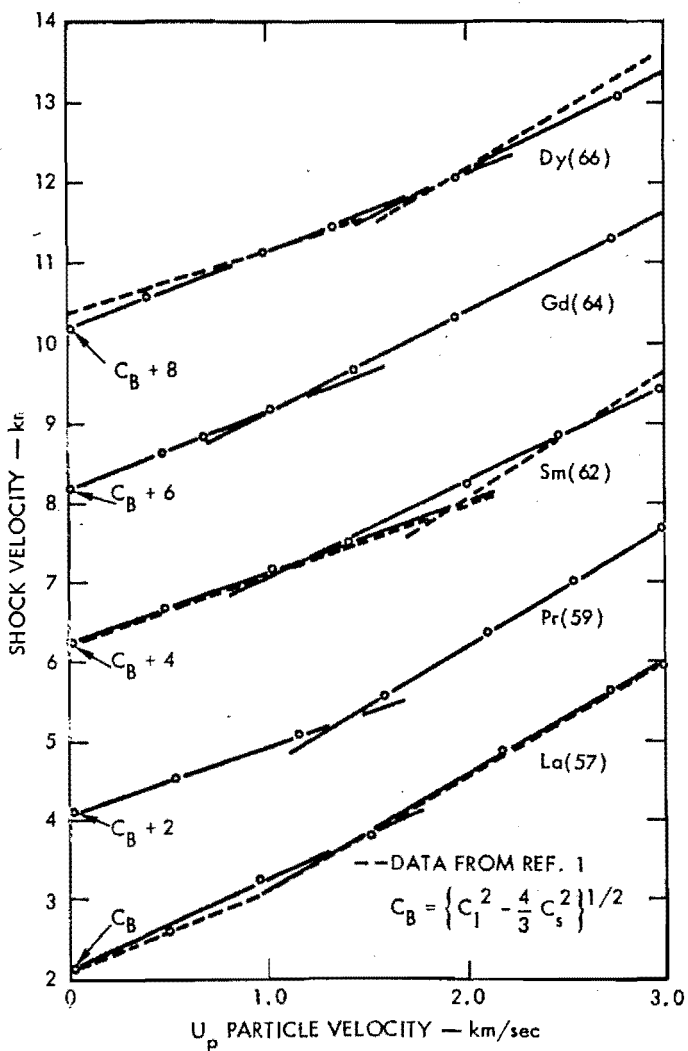


Fig. 1. Shock velocity - particle velocity Hugoniot data for five rare-earth metals. Dashed lines are fits to data from Ref. 1.

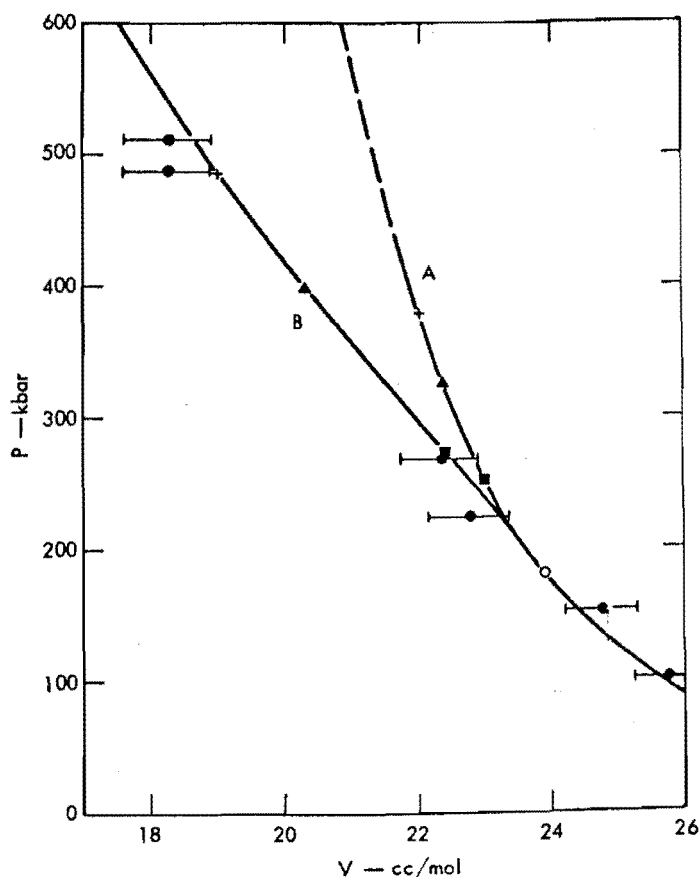


Fig. 2. Experimental measurements and theoretical calculations of Hugoniot for argon and xenon. The law of corresponding states was used to scale the argon results up to xenon. Curve A is the scaled argon experimental curve extended by theoretical calculations. Curve B is based on the xenon band calculations. Calculated Hugoniot temperatures on the two curves are  $0, 8,000^{\circ}\text{K}$ ,  $12,000^{\circ}\text{K}$ ,  $16,000^{\circ}\text{K}$ , and  $18,000^{\circ}\text{K}$ .

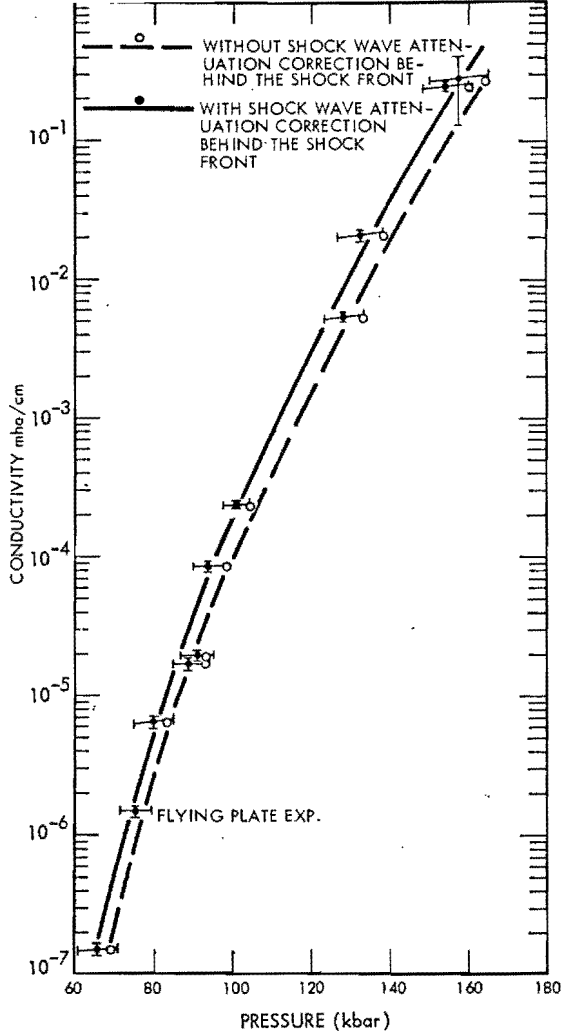
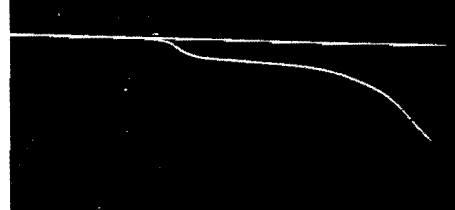
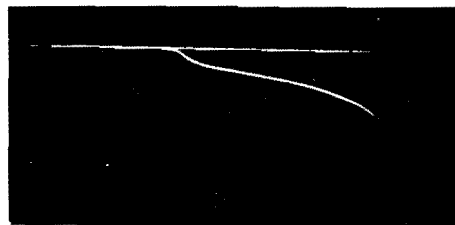


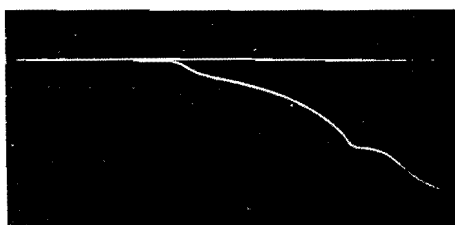
Fig. 3. Electrical conductivity of shock-compressed  $\text{CCl}_4$ .



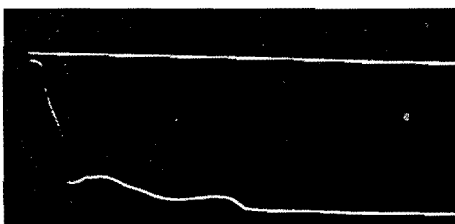
(a)



(b)



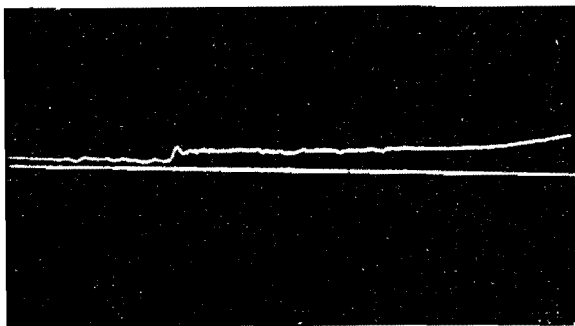
(c)



(d)

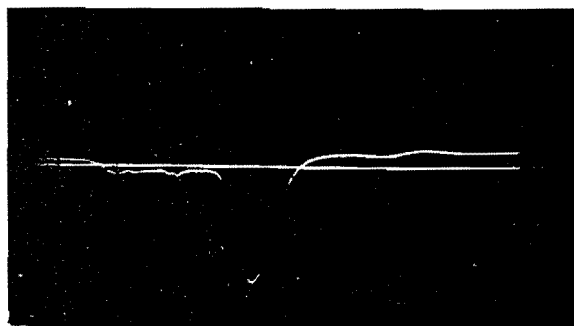
Fig. 4. The effect of shock wave reflection from a metal anvil on electrical conductivity records. a. Calcium, b. Magnesium, c. Aluminum, d. Copper. The first three records have a sweep duration of  $2 \mu\text{sec}$ ; the last has a duration of  $10 \mu\text{sec}$ .

Copper



Pressure - 260 kbar

Iron



Pressure - first wave 80 kbar  
second wave 175 kbar

Fig. 5. Conductivity records for copper and iron. Total sweep duration of both records is  $1 \mu\text{sec}$ .

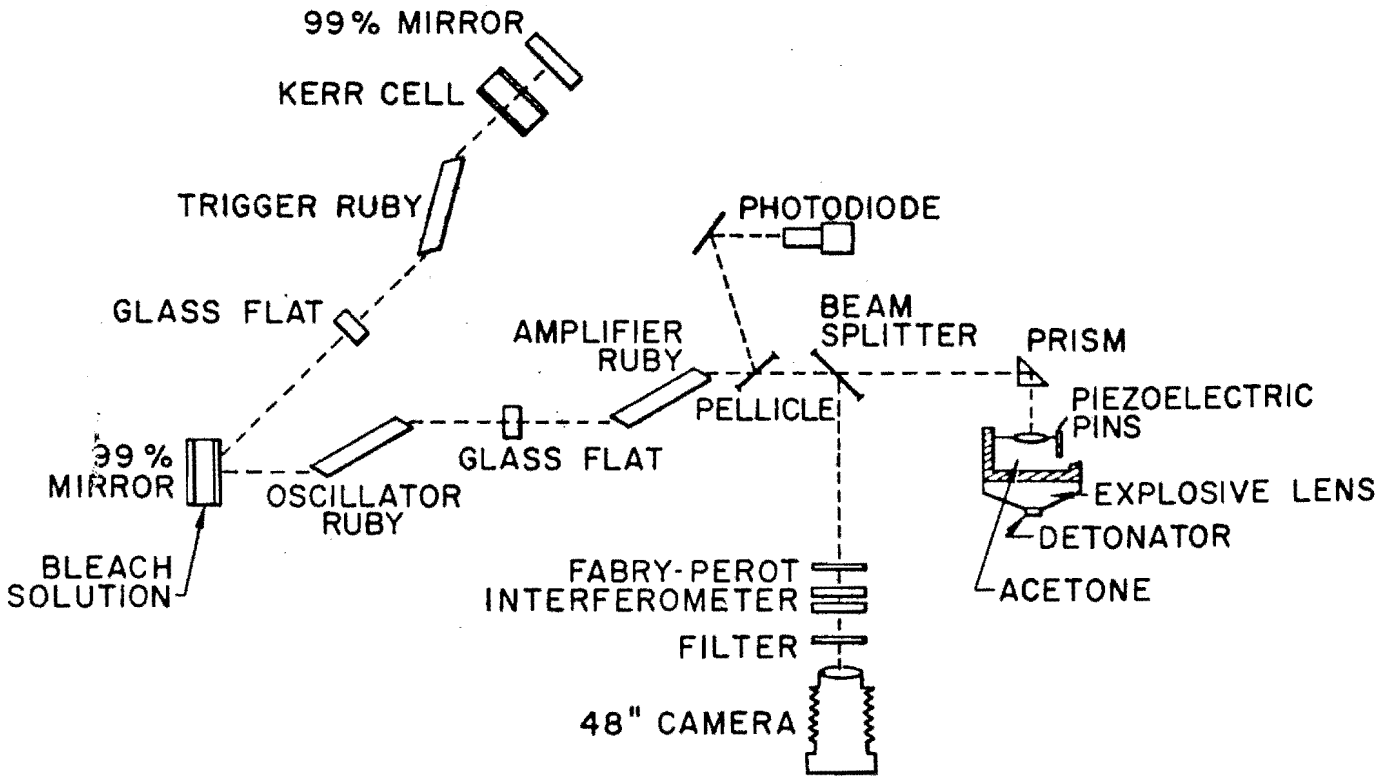


Fig. 6. Three-laser system used to observe stimulated Brillouin Scattering behind a shock wave.

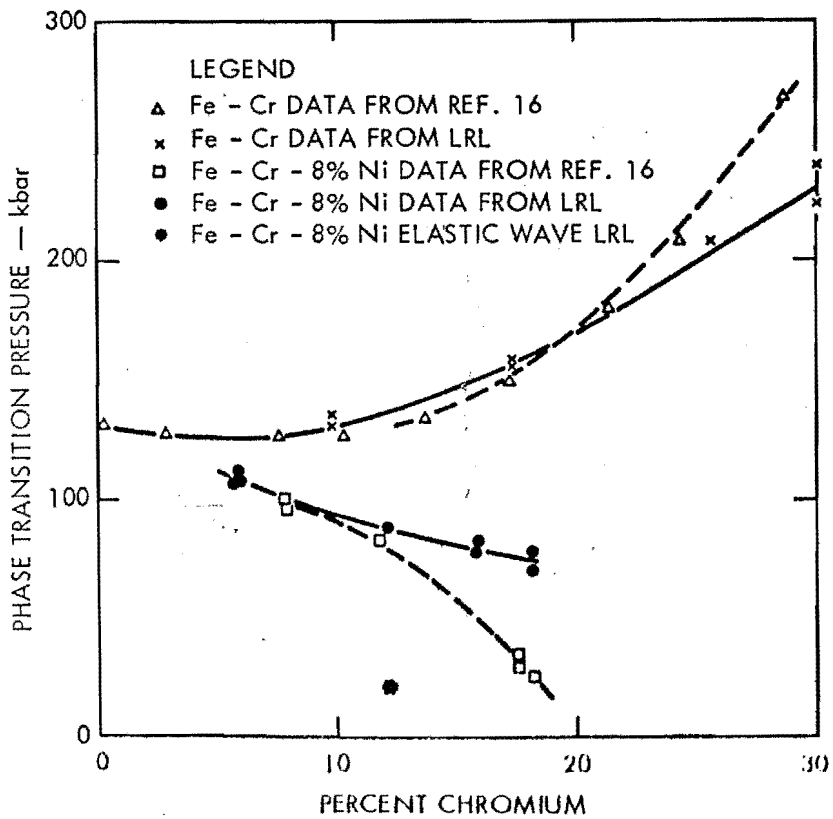


Fig. 7. Phase transition pressures for several iron-chromium and iron-chromium-nickel alloys.

## DISTRIBUTION

### LRL Internal Distribution

R. Duff

10

TID File

2

#### LEGAL NOTICE

This report was prepared as an account of Government sponsored work. Neither the United States, nor the Commission, nor any person acting on behalf of the Commission:

A. Makes any warranty or representation, expressed or implied with respect to the accuracy, completeness, or usefulness of the information contained in this report, or that the use of any information, apparatus, method, or process disclosed in this report may not infringe privately owned rights; or

B. Assumes any liabilities with respect to the use of, or for damages resulting from the use of any information, apparatus, method or process disclosed in this report.

As used in the above, "person acting on behalf of the Commission" includes any employee or contractor of the Commission, or employee of such contractor, to the extent that such employee or contractor of the Commission, or employee of such contractor, prepares, disseminates or provides access to, any information pursuant to his employment or contract with the Commission, or his employment with such contractor.

VM/lc